IDŐJÁRÁS

Quarterly Journal of the Hungarian Meteorological Service
Vol. 110, No. 3-4, July-December 2006, pp. 349-363

Description and evaluation of a coupled Eulerian transport-exchange model Part I. Model development

István Lagzi[1], Róbert Mészáros[2*], Ferenc Ács[2], Alison S. Tomlin[3], László Haszpra[4] and Tamás Turányi[1]

[1]*Department of Physical Chemistry, Institute of Chemistry, Eötvös Loránd University, P.O. Box 32, H-1518 Budapest, Hungary*

[2]*Department of Meteorology, Eötvös Loránd University, P.O. Box 32, H-1518 Budapest, Hungary; E-mail: mrobi@nimbus.elte.hu*

[3]*Energy and Resources Research Institute, University of Leeds, Leeds, LS2 9JT, U.K.*

[4]*Hungarian Meteorological Service, P.O. Box 39, H-1675 Budapest, Hungary*

(Manuscript received in final form June 22, 2006)

Abstract—An Eulerian photochemical reaction-transport model and a detailed dry deposition model have been coupled to describe both continuous air pollution and accidental release over Central Europe. Up to now, model applications have been carried out for estimating ozone flux over Hungary and transport of passive tracers from a point source. Simulating the chemical reactions, the simple GRS (Generic Reaction Set) chemical scheme was used, although, the model allows the utilization of any other, more comprehensive reaction scheme. During the transmission processes of radioactive tracers, only radioactive decay has been considered. Because of detailed parameterization of deposition processes, not only the concentration, but the effective ozone load can also be estimated by the model. Meteorological data utilized in the model have been obtained by the ALADIN meso-scale limited area numerical weather prediction model used by the Hungarian Meteorological Service. Detailed model description is presented in this study. Model sensitivity tests and some results will be presented in a companion paper.

Key-words: dispersion model, dry deposition model, adaptive grid, photochemical air pollution

* Corresponding author

1. Introduction

Previous EUROTRAC investigations (EUROTRAC 1 and EUROTRAC 2; *Haszpra et al.*, 2003) have shown that some of the highest regional ozone concentrations in Europe can be observed in Central Europe, including Hungary. During summer ozone episodes, the ozone burden of natural and agricultural vegetation is often well beyond tolerable levels. Elevated ozone concentration can be harmful to agricultural and natural vegetation. Air quality measures based on accumulated exposure over a threshold (AOT) such as AOT40 were therefore developed based on experiments in order to try to mitigate damage (*Fuhrer et al.*, 1997). However, since ozone enters plants through the stomata, the response of vegetation to changes in atmospheric ozone concentrations is more directly influenced by the stomatal ozone flux than the atmospheric concentration itself. Therefore, it has been suggested that the stomatal ozone flux is a more appropriate measure for ozone damage than the AOT 40 value (e.g., *Emberson et al.*, 2000a; *Musselman et al.*, 2006). This flux depends on several factors including the soil wetness state in moderate soil water availability conditions. An important tool in the management of photochemical smog episodes is a computational model, which can be used to test the effect of possible emission control strategies. High spatial resolution of such a model is important to reduce the impact of numerical errors on predictions and to allow better comparison of the model with experimental data during validation. The review paper of *Peters et al.* (1995) highlights the importance of developing more efficient grid systems for the next generation of air pollution models, in order to capture important smaller scale atmospheric phenomena.

This paper, therefore, presents the development of an adaptive grid model for the Central European region describing the formation of photochemical oxidants and ozone fluxes based on unstructured grids. The initial base grid of the model uses a nested approach with a coarse grid covering the wider Central European region and finer resolution grid over Hungary. Further refinement or de-refinement is then invoked using indicators based on the comparison of high and low order numerical solution of the atmospheric diffusion equation. Using this method, an efficient grid resolution strategy can be achieved in a computationally effective way.

Flux calculations without using a transport model are less precise, because of the inaccurately known spatial distribution of ozone concentrations estimated from measurements at Hungarian monitoring stations. At the same time, the spatial distribution of ozone concentration is shown to be a less accurate measure of effective ozone load, than the spatial distribution of ozone flux.

This model is also able to predict the dispersion of passive tracers (e.g., radioactive substances, chemical toxic species). The numerical algorithms applied in this version of the dispersion model are based on SPRINT2D software package (*Berzins et al.*, 1989; *Berzins* and *Furzeland,* 1992; *Berzins* and *Ware,* 1995, 1996).

Input data for the coupled transport–deposition model are presented in *Table 1*. Detailed description of both transport and deposition models is presented in next chapters.

Table 1. Input data of the model

	Input data	Notation	Unit
Place and time	Latitude, longitude	φ, λ	radian
	Elevation	z_a	m
	Season categories	S_x	-
	Day of the year	D_y	-
	Hour	t_{UTC}	hour
Surface atmospheric data	Air temperature	t_a	°C
	Components of wind speed	u, v	m s^{-1}
	Global radiation	R_G	W m^{-2}
	Cloudiness	N	eighth
	Relative humidity	f	%
	Daily precipitation amount	P	mm
Upper air meteorological data	Air temperature (4 layers)	t_a	°C
	Components of wind speed (4 layers)	u, v	m s^{-1}
	Relative humidity (4 layers)	f	%
	Height of the mixing layer	H_m	m
Emission inventories	NO_x, VOC, CO	E_i	g s^{-1}
Surface and plant specific parameters	Land use categories	LUC	-
	Height of vegetation	z_{veg}	m
	Roughness length	z_0	m
	Displacement height	d	m
	Albedo	A	-
	Leaf area index	LAI	m^2 m^{-2}
	Modified Pristley-Taylor parameter	α	-
Soil parameters	Soil categories	Tx	-
	Field capacity soil moisture content	θ_f	m^3 m^{-3}
	Wilting point soil moisture content	θ_w	m^3 m^{-3}
	Saturated soil moisture content	θ_s	m^3 m^{-3}
Resistance parameters	Minimum stomatal resistance	$r_{st\,min}$	s m^{-1}
	Radiation correction term	b_{st}	W m^{-2}
	Minimum temperature	t_{min}	°C
	Maximum temperature	t_{max}	°C
	Optimal temperature	t_{opt}	°C
	Mesophyll resistance	R_{mes}	s m^{-1}
	Cuticular resistance	R_{cut}	s m^{-1}
	Soil resistance	R_s	s m^{-1}

2. *The dispersion model*

The model describes the spread of reactive air pollutants within a 2D unstructured triangular based grid representing layers within the troposphere over the Central European region, including Hungary. The model describes the horizontal domain using a Cartesian coordinate system through the stereographic polar projection of a curved surface onto a flat plane. The total horizontal domain size is 1540 km × 1500 km (*Fig. 1*). Vertical resolution of pollutants is approximated by the application of four layers representing the surface, mixing, reservoir layers and the free troposphere. Reactive dispersion in the horizontal domain is described by the atmospheric diffusion equation in two space dimensions:

$$\frac{\partial c_s}{\partial t} = -\frac{\partial (u c_s)}{\partial x} - \frac{\partial (v c_s)}{\partial y} + \frac{\partial}{\partial x}\left(K_x \frac{\partial c_s}{\partial x}\right) + \frac{\partial}{\partial y}\left(K_y \frac{\partial c_s}{\partial y}\right) + R_s(c_1, c_2, \ldots, c_n) + E_s - k_s c_s, \tag{1}$$

where c_s is the concentration of the *s*th compound, u and v are horizontal wind components, K_x and K_y are eddy diffusion coefficients, k_s is the dry deposition rate constant, E_s describes the distribution of emission sources for the *s*th compound, and R_s is the chemical reaction term, which may contain non-linear terms in c_s. For n chemical species, an n dimensional set of partial differential equations is formed describing the change of concentrations over time and space. These equations are coupled through the non-linear chemical reaction term.

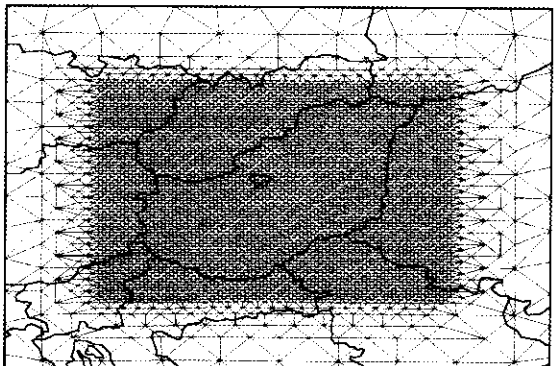

Fig. 1. The typical nested grid structure of the dispersion model. The average mesh length of the outer coarse grid and that of the nested fine grid are 100 and 12.5 km, respectively.

The four vertical layers of the model are defined as: the surface layer extending to 50 m, the mixing layer, a reservoir layer, and the free troposphere (upper) layer. The mixing layer extends to a height determined by radiosonde data at 00:00 UTC, but is modeled to rise smoothly to a height determined by radiosonde data at 12:00 UTC during the day. The reservoir layer, if it exists above the height of the mixing layer, extends from the top of the mixing layer to an altitude of 1000 m.

Relative humidity and temperature data were determined by the meteorological model ALADIN with a time resolution of 6 hours and spatial resolution of 0.1×0.15 degrees (*Horányi et al.*, 1996). In our model, conservative interpolation methods were used to obtain data relevant to a given spatial point on the unstructured grid from the regularly gridded ALADIN meteorological data.

For Budapest, the emission inventories for CO, NO_x, and VOCs were provided by the local authorities with a spatial resolution of 1 km × 1 km including the most significant 63 emission point sources. For Hungary, the National Emission Inventory of spatial resolution of 20 km × 20 km was applied, which included both area and point sources. Outside Hungary, the emission inventory of EMEP for CO, NO_x, and VOCs was used, having a spatial resolution of 50 km × 50 km. Natural VOC and NO_x emission have been neglected in the model. Parameterization of biogenic emissions requires several other input data, such as forest statistical data and bibliographic data on three species potential emissions. However, based on the study of *Moukhtar et al.* (2005), the effect of biogenic emissions of ozone precursors (VOC) on ozone concentration was only maximum 5%.

The emission data had to be interpolated onto the unstructured grid following each change to the mesh during refinement. This was achieved using the mass conservative method of overlapping triangles. Point sources are averaged into the appropriate grid cell for their location, and hence, when the grid is refined, the definition of point sources improves.

In the model, the GRS chemical scheme (*Azzi et al.*, 1992; *Cope et al.*, 2005) was used, although the model allows the utilization of any other reaction schemes. The GRS scheme is a reduced mechanism that was created using a semi-empirical approach; it contains 7 reactions of 7 species (*Table 2*). The GRS scheme has been evaluated by comparison with smog chamber data and predictions from more detailed chemical schemes. Previous studies (*Azzi et al.*, 1992; *Cope et al.*, 2005) have shown that the scheme performs well for the prediction of ozone in polluted conditions, although it can overpredict ozone concentrations in rural locations. The scheme has been selected in the current application for its computational efficiency, and because its accuracy can be assumed to be reasonable in the region of interest, i.e., down wind of major

NO_x sources. The rate constants were calculated and expressed as *m*th order rate constants with units (molecule $cm^3)^{m-1}$ s^{-1}. The photolysis rates were parameterized by the following function:

$$J_q = (1 - 0.75N^{3.4})a_q \exp(b_q \sec \Theta), \quad (2)$$

where Θ is the solar zenith angle, N is the cloud coverage, and a_q, b_q are the rate parameters of reaction q. Temperature dependent rate constants were represented by standard Arrhenius expressions.

Table 2. The GRS mechanism (T: temperature, Θ: solar zenith angle)

Reactions	Reaction rate constants	
ROC + $h\nu$ $\rightarrow$ RP + ROC	$k_1 = 1000 \exp(-4710/T) J_3$	[R1]
RP + NO $\rightarrow$ NO_2	$k_2 = 3.7098 \times 10^{-12} \exp(242/T)$	[R2]
NO_2 + $h\nu$ $\rightarrow$ NO + O_3	$J_3 = 1.45 \times 10^{-2} \exp(-0.4 \sec \Theta)$	[R3]
NO + O_3 $\rightarrow$ NO_2	$k_4 = 1.7886 \times 10^{-12} \exp(-1370/T)$	[R4]
RP + RP $\rightarrow$ RP	$k_5 = 6.7673 \times 10^{-12}$	[R5]
RP + NO_2 $\rightarrow$ SGN	$k_6 = 1.00 \times 10^{-13}$	[R6]
RP + NO_2 $\rightarrow$ SNGN	$k_7 = 1.00 \times 10^{-13}$	[R7]

2.1 Solution method

The basis of the numerical method is the space discretization of the partial differential equations (PDEs) derived from the atmospheric diffusion equation on unstructured triangular meshes using the software SPRINT2D (*Berzins et al.*, 1989; *Berzins* and *Furzeland,* 1992; *Berzins* and *Ware*, 1995, 1996). This approach (known as the "method of lines"), reduces the set of PDEs in three independent variables to a system of ordinary differential equations (ODEs) in one independent variable, the time. The system of ODEs can then be solved as an initial value problem. For advection dominated problems it is important to choose a discretization schemes which preserves the physical range of the solution.

Unstructured triangular meshes are commonly used in finite volume/element applications because of their ability to deal with general geometries. In terms of application to multi-scale atmospheric problems, we are not dealing with complex physical geometries, but unstructured meshes provide a good method of resolving the complex structures formed by the interaction of chemistry and flow in the atmosphere and by the varying types of emission sources. The term unstructured represents the fact that each node in the mesh may be surrounded by any number of triangles, whereas in a structured mesh this number would be fixed. In the present work, a flux limited, cell-centered, finite volume discretization scheme of *Berzins* and *Ware* (1995, 1996) was chosen on an unstructured triangular mesh. This method enables accurate solutions to be determined for both smooth and discontinuous flows by making use of the local Riemann solver flux techniques (originally developed for the Euler equations) for the advective parts of the fluxes, and centered schemes for the diffusive part. The scheme of *Berzins* and *Ware* (1995, 1996) has the desirable properties of preserving positivity, eliminating spurious oscillations, and restricting the amount of diffusion by the use of a nonlinear limiter function. The advection scheme has been shown to be of second order accuracy. The diffusion terms are discretized by using a finite volume approach to reduce the integrals of second derivatives to the evaluation of first derivatives at the midpoints of edges. These first derivatives are then evaluated by differentiating a bilinear interpolant based on four mid-point values. The model applies Dirichlet- and Neumann-type boundary conditions depending on the advective fluxes over boundary edge. The boundary conditions are imposed through the approximate Riemann solver.

A method of lines approach with the above spatial discretization scheme results in a system of ODEs in time, which are integrated using the code SPRINT with the Theta option ,which is specially designed for the solution of stiff systems with moderate accuracy and automatic control of the local error in time. Operator splitting is carried out at the level of the nonlinear equations formed from the method of lines by approximating the Jacobian matrix. The approach introduces a second-order splitting error, but fortunately this error alters only the rate of convergence of the iteration, as the residual being reduced is still that of the full ODE system. This provides significant advantages over other splitting routines such as Strang splitting.

The initial unstructured meshes used in SPRINT2D are created from a geometry description using the Geompack mesh generator (*Joe*, 1991). These meshes are then refined and coarsened by the Triad adaptivity module, which uses tree like data structures to enable efficient mesh adaptation by providing the necessary connectivity. A method of refinement based on the regular subdivision of triangles has been chosen. Here an original triangle is split into four similar triangles by connecting the midpoints of the edges as shown in *Fig. 2*. These may be coalesced into the parent triangle later, when coarsening the mesh. This process is called local h-refinement, since the nodes of the original mesh do not move, and we are simply subdividing the original elements. In order to implement the adaptivity module, a suitable criterion must be chosen. The ideal situation would be that the decision to refine or de-refine would be made on a fully automatic basis with no user input necessary.

In practice, a combination of an automatic technique and some knowledge of the physical properties of the system is used. The technique used in this work is based on the calculation of spatial error estimates. Low and high order solutions are obtained for each species, and the difference between them gives a measure of the spatial error. The algorithm can then be choosen to refine in regions of high spatial error by comparison with a user defined tolerance for one or the sum of several species. For the *i*th PDE component on the *j*th triangle, a local error estimate $e_{i,j}(t)$ is calculated from the difference between the solution using a first order method and that using a second order method. For time dependent PDEs, this estimate shows how the spatial error grows locally over a time step. A refinement indicator for the *j*th triangle is defined by an average scaled error ($serr_j$) measurement over all *npde* PDEs using supplied absolute and relative tolerances:

$$serr_j = \sum_{i=1}^{npde} \frac{e_{i,j}(t)}{atol_i / A_j + rtol_i \, c_{i,j}}, \tag{3}$$

where $atol_i$ and $rtol_i$ are the absolute and relative error tolerances, $e_{i,j}(t)$ is the local error estimate of species i over element j, $c_{i,j}$ is the concentration of species i over triangle, j, A_j is the area of *j*th triangle and *npde* is the number of partial differential equations applied. This formulation for the scaled error provides a flexible way to weight the refinement towards any PDE errors.

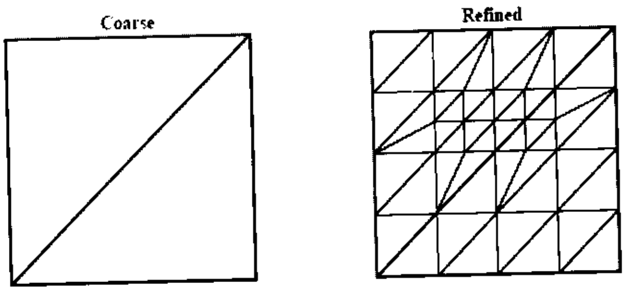

Fig. 2. Subdivision of the triangular cells using adaptive gridding strategy.

In the photochemical smog calculations, a combination of errors in species NO and NO_2 were used as a refinement indicator, because these are primary species, and also because their concentrations are very closely related to ozone production. Estimation of the local spatial error of ozone concentration is not an efficient choice, because it would be too late to make refinement decisions on the basis of the detection of a large error in the concentration of a secondary pollutant. On the other hand, concentrations of the VOCs are locally dominated by emissions, and since the available emission inventory for VOCs has a coarse resolution (50 km × 50 km), the use of VOC concentration as an error indicator is not appropriate. *Tomlin et al.* (1997) previously demonstrated the success of using the local spatial error of the concentrations of nitrogen oxides for appropriate mesh refinement for a reactive plume from a NO_x ($NO+NO_2$) source. Each triangle that is flagged for refinement is split into four similar triangles (*Fig. 2*). Refined triangles may later be coalesced into the parent triangle when coarsening the mesh.

The application of adaptive rectangular meshes would be also possible but less effective in terms of the number of nodes required in order to achieve high levels of adaptivity. Although the data structures resulting from an unstructured mesh are somewhat more complicated than those for a regular Cartesian mesh, problems with hanging nodes at boundaries between refinement regions are avoided. The use of a flexible discretization stencil also allows for an arbitrary degree of refinement, which is more difficult to achieve on structured meshes.

3. The dry deposition model

Models to describe the dry deposition of ozone are based on the inferential method (*Baldocchi et al.*, 1987; *Hicks et al.*, 1987; *Kramm et al.*, 1995; *Padro*, 1996; *Walmsley* and *Wesely*, 1996; *Grünhage* and *Haenel*, 1997; *Meyers et al.*, 1998; *Padro et al.*, 1998; *Brook et al.*, 1999; *Emberson et al.*, 2000b; *Klemm* and *Mangold*, 2001; *Zhang et al.*, 2002). The dry deposition velocity of ozone was estimated over different types of vegetation. The land-cover map was generated using a Hungarian land-use map (*Fig. 3*). The model was applied on the grid of the meso-scale limited area numerical weather prediction model ALADIN (*Horányi et al.*, 1996). The time and space resolution of the data was 6 hours and 0.10 × 0.15 degrees, respectively.

The total ozone flux (F_t) was calculated as a product of the deposition velocity of ozone (v_d) and the ozone concentration (c_r) at a reference height (within the surface layer of the model):

$$F_t = v_d \, c_r \tag{4}$$

The deposition velocity is defined as the inverse of the sum of the atmospheric and surface resistances, which retard the ozone flux:

$$v_d = (R_a + R_b + R_c)^{-1}, \tag{5}$$

where R_a, R_b, and R_c are the aerodynamic resistance, the quasi-laminar boundary layer resistance, and the canopy resistance, respectively.

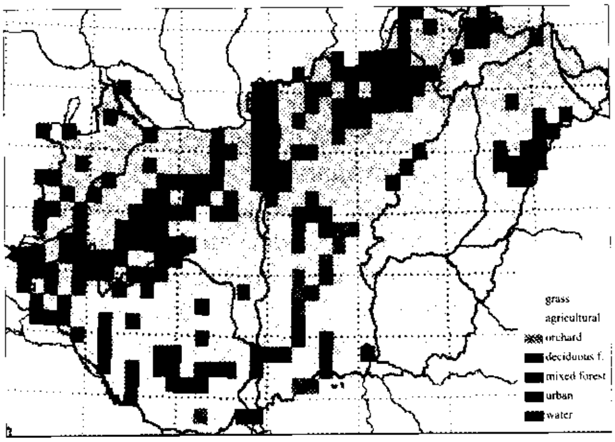

Fig. 3. Land use categories in the model.

The aerodynamic resistance is calculated using the Monin-Obukhov similarity theory taking into account the atmospheric stability (*Ács* and *Szász*, 2002):

$$R_a = \frac{1}{\kappa u_*} \ln\left(\frac{z-d}{z_0}\right) + 4.7\frac{z-d-z_0}{L} \quad \text{if } L > 0, \tag{6}$$

and

$$R_a = \frac{1}{\kappa u_*} \ln\left(\frac{1-y}{1-y_0}\frac{1+y_0}{1+y}\right) \quad \text{if } L < 0, \tag{7}$$

where

$$y = \left(1 - 16\frac{z-d}{L}\right)^{-1/2}, \tag{8}$$

$$y_0 = \left(1 - 16\frac{z_0}{L}\right)^{-1/2}, \tag{9}$$

where z, z_0, and d are the reference height, the roughness length, and the displacement height, respectively, depending on the surface types, $\kappa = 0.4$ is the von Kármán constant. Dynamical parameters, such as u_* and L are the friction velocity and the Monin-Obukhov length, respectively, calculated by an iterative method:

$$u_* = \kappa u \left[\ln\left(\frac{z-d}{z_0}\right) - \psi_m\left(\frac{z-d}{L}\right) + \psi_m\left(\frac{z_0}{L}\right) \right]^{-1}, \tag{10}$$

and

$$L = -\frac{u_*^3 \rho c_p T}{\kappa g H}, \tag{11}$$

where $\psi_m(\xi)$ is the integral form of universal stability correction functions for the momentum, g is the acceleration of gravity, ρ is the air density, c_p is the specific heat at constant pressure, T is the air temperature, and H is the sensible heat flux. In this study, universal functions for wind of *Beljaars* and *Holtslag* (1991) and *Dyer* (1974) were used for stable and unstable stratifications, respectively. The sensible heat flux was estimated using the modified Priestley-Taylor method (*Holtslag* and *van Ulden*, 1983).

The boundary layer resistance for ozone is calculated by an empirical relationship after *Hicks et al.* (1987):

$$R_b = 6.5 / u_* . \tag{12}$$

The canopy resistance R_c is parameterized by the following equation:

$$R_c = \frac{1}{(R_{st} + R_{mes})^{-1} + (R_s)^{-1} + (R_{cut})^{-1}}, \tag{13}$$

where R_{st}, R_{mes}, R_s, and R_{cut} are the stomatal, mesophyll, surface, and cuticular resistances, respectively.

The stomatal resistance can be calculated from the empirical formula of *Jarvis* (1976) referring to a vegetation canopy. This parameterization requires knowledge of the soil and plant physiological characteristics:

$$R_{st} = \frac{1}{G_{st}(PAR) f_t(t) f_e(e) f_\theta(\theta) f_{D,i}}, \tag{14}$$

where $G_{st}(PAR)$ is the unstressed canopy stomatal conductance, a function of PAR, the photosynthetically active radiation. In this parameterization, the canopy is divided into sunlit and shaded leaves, and G_{st} is calculated with the following form:

$$G_{st}(PAR) = \frac{LAI_s}{r_{st}(PAR_s)} + \frac{LAI_{sh}}{r_{st}(PAR_{sh})}, \tag{15}$$

$$r_{st}(PAR) = r_{st,\min}(1 + b_{st} / PAR), \tag{16}$$

where LAI_s and LAI_{sh} are the total sunlit and shaded leaf area indices, respectively, PAR_s and PAR_{sh} are PAR received by sunlit and shaded leaves, respectively. LAI_s, LAI_{sh}, PAR_s, and PAR_{sh} terms are parameterized after *Zhang et al.* (2001). The vegetation specific terms $r_{st,\min}$, b_{st}, and LAI are presented in *Lagzi et al.* (2004).

The factors in the denominator range between 0 and 1 and modify the stomatal resistance: $f_t(t)$, $f_e(e)$, and $f_\theta(\theta)$ describe the effect of temperature, the vapor pressure deficit, and plant water stress on stomata, while $f_{D,i}$ modifies the stomatal resistance for the pollutant gas of interest (for ozone, $f_{D,i} = 0.625$ after *Wesely* (1989)).

The temperature stress function is described by the following equation:

$$f_t = \frac{t - t_{\min}}{t_{opt} - t_{\min}} \left(\frac{t_{\max} - t}{t_{\max} - t_{opt}} \right)^{b_t}, \tag{17}$$

where

$$b_t = \frac{t_{\max} - t_{opt}}{t_{\max} - t_{\min}}. \tag{18}$$

Here $t_{\min}, t_{opt}$, and $t_{\max}$ are the minimum, maximum, and the optimal temperature depending on the vegetation. The stress of the vapor pressure deficit can be parameterized by the following form:

$$f_e = 1 - b_e(e_s - e), \tag{19}$$

where b_e is a vegetation dependent constant (*Brook et al.*, 1999), e and e_s are the water vapor pressure and the saturated water vapor pressure, respectively.

The water stress function $f_\theta(\theta)$ is parameterized using soil water content (θ):

$$f_\theta = \begin{cases} 1 & if\,\theta > \theta_f \\ \max\left\{ \dfrac{\theta - \theta_w}{\theta_f - \theta_w}, 0.05 \right\} & if\,\theta_w < \theta \le \theta_f \\ 0.05 & if\,\theta \le \theta_w \end{cases}, \tag{20}$$

where θ_w and θ_f are the wilting point and the field capacity soil moisture contents, respectively. These terms depend on the soil texture of the grid cell. The soil texture on the model grid was determined after *Várallyay et al.*

(1980). The grid cell soil texture was represented by the dominant soil texture (*Fig. 4*). The θ_w and θ_f values for several soil textures were taken from *Ács* (2003). Soil water content, θ, was modeled by a simple water-budget model (*Mészáros et al.*, 2006).

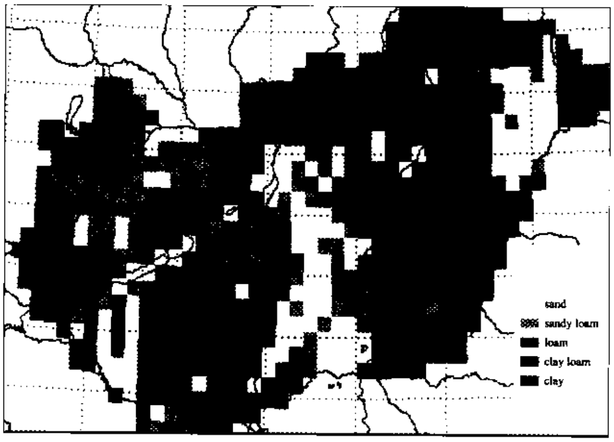

Fig. 4. Soil types in the model.

The mesophyll resistance for ozone in the model is taken to be zero. Cuticular resistance, R_{cut}, and surface resistance, R_s, for ozone deposition were obtained as in *Lagzi et al.* (2004). The calculated deposition velocities of ozone over different vegetation have a good agreement with published observed data (see *Lagzi et al.*, 2004).

4. Conclusions

A chemical transport model and a detailed dry-deposition model have been developed and coupled to simulate the ozone fluxes over the Central European region and estimate the dispersion of an accidental release from the nuclear power plant at Paks, Hungary. An adaptive grid model describes the formation and transformation of photochemical oxidants based on triangular unstructured grids. The model automatically places a finer resolution grid in regions characterized by high concentration gradients and, therefore, higher numerical error. Using an adaptive method, it is therefore possible to achieve grid resolutions of the order of 10 km without excessive computational effort.

Sensitivity tests and model results are presented in the second part of this study.

Acknowledgements—The authors acknowledge the support of OTKA D048673 (Postdoctoral Fellowship), OTKA F047242, NKFP 3A/088/2004, and the Békésy György Fellowship.

References

Ács, F., 2003: On the relationship between the spatial variability of soil properties and transpiration. *Időjárás 107*, 257–272.

Ács, F. and *Szász, G.*, 2002: Characteristics of microscale evapotranspiration: a comparative analysis. *Theor. Appl. Climatol. 73*, 189–205.

Azzi, M., *Johnson, G.J.*, and *Cope, M.*, 1992: An introduction to the generic reaction set photochemical smog mechanism. *Proceedings of the 11th Clean Air Conf. 4th Regional IUAPPA Conf.*, Brisbane, Australia, pp. 451–462.

Baldocchi, D.D., *Hicks, B.B.*, and *Camara, P.*, 1987: A canopy stomatal resistance model for gaseous deposition to vegetated canopies. *Atmos. Environ. 21*, 91–101.

Beljaars, A.C.M. and *Holtslag, A.A.M.*, 1991: Flux parameterization overland surfaces for atmospheric models. *J. Appl. Meteorol. 30*, 327–341.

Berzins, M., *Dew, P.M.*, and *Furzeland, R.M.*, 1989: Developing software for time-dependent problems using the method of lines and differential algebraic integrators. *Appl. Numer. Math. 5*, 375–390.

Berzins, M. and *Furzeland, R.M.*, 1992: An adaptive Theta-method for the solution of stiff and nonstiff differential-equations. *Appl. Numer. Math. 9*, 1–19.

Berzins, M. and *Ware, J.*, 1995: Positive cell-centered finite volume discretization methods for hyperbolic equations on irregular meshes. *Appl. Numer. Math. 16*, 417–438.

Berzins, M. and *Ware, J.*, 1996: Solving convection and convection reaction problems using the method of lines. *Appl. Numer. Math. 20*, 83–99.

Brook, J.R., *Zhang, L.*, *Di-Giovanni, F.*, and *Padro, J.*, 1999: Description and evaluation of a model of deposition velocities for routine estimates of air pollutant dry deposition over North America. Part I: model development. *Atmos. Environ. 33*, 5037–5051.

Cope, M.E., *Hess, G.D.*, *Lee, S.*, *Tory, K.J.*, *Burgers, M.*, *Dewundege, P.*, and *Johnson, M.*, 2005: The Australian Air Quality Forecasting System: Exploring first steps towards determining the limits of predictability for short-term ozone forecasting. *Bound.-Lay. Meteorol. 116*, 363–384.

Dyer, A.J., 1974: A review of flux-profile relationships. *Bound.-Lay. Meteorol. 7*, 363–372.

Emberson, L.D., *Simpson, D.*, *Tuovinen, J.-P.*, *Ashmore, M.R.*, and *Cambridge, H.M.*, 2000a: Towards a model of ozone deposition and stomatal uptake over Europe. *EMEP MSC-W Note 6/00.*

Emberson, L.D., *Ashmore, M.R.*, *Cambridge, H.M.*, *Simpson, D.*, and *Touvinen, J.-P.*, 2000b: Modelling stomatal ozone flux across Europe. *Atmos. Environ. 109*, 403–413.

Fuhrer, J., *Skärby, L.*, and *Ashmore, M.R.*, 1997: Critical levels for ozone effects on vegetation in Europe. *Environ. Pollut. 97*, 91–106.

Grünhage, L. and *Haenel, H.D.*, 1997: PLATIN (PLant-ATmosphere INteraction) I: a model of plant-atmosphere interaction for estimating absorbed doses of gaseous air pollutants. *Environ. Pollut. 98*, 37–50.

Haszpra, L., *Ferenczi, Z.*, *Lagzi, I.*, and *Turányi, T.*, 2003: Formation of Tropospheric Ozone Formation in Hungary. In *EUROTRAC-2 (A EUREKA Environmental Project) TOR-2 Tropospheric Ozone Research. Final Report.* International Scientific Secretariat (ISS), GSF - National Research Center for Environment and Health, Munich, 87–89.

Hicks, B.B., *Baldocchi, D.D.*, *Meyers, T.P.*, *Hosker, R.P.*, and *Matt, D.R.*, 1987: A preliminary multiple resistance routine for deriving dry deposition velocities from measured quantities. *Water Air Soil Poll. 36*, 311–330.

Holtslag, A.A.M. and *van Ulden, A.P.*, 1983: A simple scheme for datetime estimates of the surface fluxes from routine weather data. *J. Clim. Appl. Meteorol. 22*, 517–529.

Horányi, A., Ihász, I., and *Radnóti, G.*, 1996: ARPEGE/ALADIN: A numerical Weather prediction model for Central-Europe with the participation of the Hungarian Meteorological Service. *Időjárás 100*, 277–301.

Jarvis, P.G., 1976: The interpretation of the variations in leaf water potential and stomatal conductance found in canopies in the field. *Phil. Trans. Roy. Soc. B 273*, 593–610.

Joe B., 1991: GEOMPACK - a software package for the generation of meshes using geometric algorithms. *Adv. Eng. Softw. Workst. 13*, 325-331.

Klemm, O. and *Mangold, A.*, 2001: Ozone deposition at a forest site in the Bavaria. *Water Air Soil Poll.: Focus 1*, 223–232.

Kramm, G., Dlugi, R., Dollard, G.J., Foken, Th., Mölders, N., Müller, H., Seiler, W., and *Sievering, H.*, 1995: On the dry deposition of ozone and reactive nitrogen species. *Atmos. Environ. 29*, 3209-3231.

Lagzi, I., Mészáros, R., Horváth, L., Tomlin, A., Weidinger, T., Turányi, T., Ács, F., and *Haszpra, L.*, 2004: Modelling ozone fluxes over Hungary. *Atmos. Environ. 38*, 6211–6222.

Mészáros, R., Szinyei, D., Vincze, Cs., Lagzi, I., Turányi,T., Haszpra, L., and *Tomlin A.S.*, 2006: Effect of the soil wetness state on the stomatal ozone fluxes over Hungary. *Int. J. Environ. Pollut.* (in press).

Meyers, T.P., Finkelstein, P., Clarke, J., Ellestad, T.G., and *Sims, P.F.*, 1998: A multilayer model for inferring dry deposition using standard meteorological measurements. *J. Geophys. Res.-Atmos. 103*, 22645–22661.

Moukhtar, S., Bessagnet, B., Rouil, L., and *Simon, V.*, 2005: Monoterpene emissions from Beech (*Fagus sylvatica)* in a French forest and impact on secondary pollutants formation at regional scale. *Atmos. Environ. 39*, 3535–3547.

Musselman, R.C., Lefohn, A.S., Massmann, W.J., and *Heath, R.L.*, 2006: A critical review and analysis of the use of exposure- and flux-based ozone indices for predicting vegetation effects. *Atmos. Environ. 40*, 1869–1888.

Padro, J., 1996: Summary of ozone dry deposition velocity measurements and model estimates over vineyard, cotton, grass and desciduous forest in summer. *Atmos. Environ. 30*, 2363–2369.

Padro, J., Zhang, L., and *Massman, W.J.*, 1998: An analysis of mesurements and modelling of air-surface exchange of NO-NO_2-O_3 over grass. *Atmos. Environ. 32*, 1167–1177.

Peters, L.K., Berkovitz, C.M., Carmichael, G.R., Easter, R.C., Fairweather, G., Ghan, S.J., Hales, J.M., Leung, L.R., Pennell, W.R., Potra, F.A., Saylor, R.D., and *Tsang T.T.*, 1995: The current and future direction of Eulerian Models in simulating the tropospheric chemistry and transport of trace species: a review. *Atmos. Environ. 29*, 189–222.

Tomlin, A., Berzins, M., Ware, J., Smith, J., and *Pilling, M.J.*, 1997: On the use adaptive gridding methods for modelling chemical transport from multi-scale sources. *Atmos. Environ. 31*, 2945–2959.

Várallyay, Gy., Szűcs, L., Murányi, A., Rajkai, K., and *Zilahy, P.*, 1980: Map of soil factors determining the agro-ecological potential of Hungary (1:100 000) II. (in Hungarian). *Agrokémia és Talajtan 29*, 35–76.

Walmsley, J.L. and *Wesely, M.L.*, 1996: Modification of coded parameterizations of surface resistances to gaseous dry deposition (Technical note). *Atmos. Environ. 30*, 1181–1188.

Wesely, M.L., 1989: Parameterization of surface resistances to gaseous dry deposition in regional-scale numerical models. *Atmos. Environ. 23*, 1293–1304.

Zhang, L., Moran, M.D., and *Brook, J.R.*, 2001: A comparison of models to estimate in-canopy photosynthetically active radiation and their influence on canopy stomatal resistance. *Atmos. Environ. 35*, 4463–4470.

Zhang, L., Moran, M.D., Makar, P.A., Brook, R., and *Gong, S.*, 2002: Modelling gaseous dry deposition in AURAMS: a unified regional air-quality modelling system. *Atmos. Environ. 36*, 537–560.